iScience

Article

Bacterial suppressor-of-copper-sensitivity proteins exhibit diverse thiol-disulfide oxidoreductase cellular functions

Graphical abstract

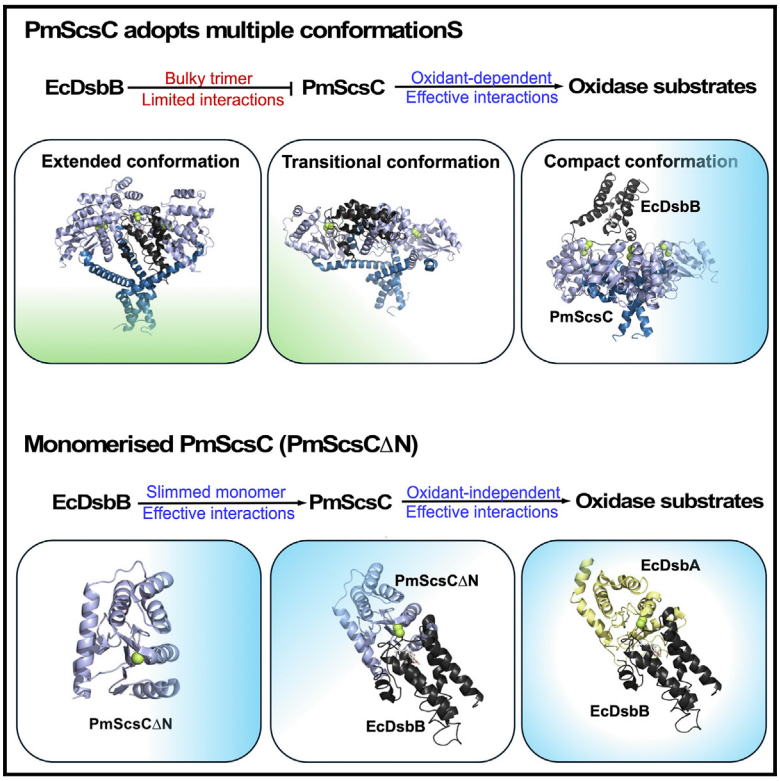

Highlights

- ScsC interacts with DsbD while avoiding DsbB to maintain its reductase function
- Oligomerization directs ScsC activity by limiting unwanted redox interactions
- Monomeric StScsC can also evade unfavorable redox pairing in the periplasm
- ScsC functions as both isomerase and oxidase, with the latter requiring exogenous oxidants

Authors

Yaoqin Hong, Jilong Qin, Lachlan Mitchell, Jason J. Paxman, Begoña Heras, Makrina Totsika

Correspondence

yaoqin.hong@jcu.edu.au (Y.H.), makrina.totsika@qut.edu.au (M.T.)

In brief

Biochemistry; Microbiology; Structural biology

Hong et al., 2024, iScience 27, 111392
December 20, 2024
https://doi.org/10.1016/j.isci.2024.111392

CellPress

iScience

CellPress
OPEN ACCESS

Article

Bacterial suppressor-of-copper-sensitivity proteins exhibit diverse thiol-disulfide oxidoreductase cellular functions

Yaoqin Hong,[1,3,4,*] Jilong Qin,[1] Lachlan Mitchell,[2] Jason J. Paxman,[2] Begoña Heras,[2] and Makrina Totsika[1,*]
[1]Centre for Immunology and Infection Control, School of Biomedical Sciences, Faculty of Health, Queensland University of Technology, Brisbane, QLD, Australia
[2]Department of Biochemistry and Genetics, La Trobe Institute for Molecular Science, La Trobe University, Bundoora, VIC, Australia
[3]Present address: College of Public Health, Medical and Veterinary Sciences, James Cook University, Townsville, Australia
[4]Lead contact
*Correspondence: yaoqin.hong@jcu.edu.au (Y.H.), makrina.totsika@qut.edu.au (M.T.)
https://doi.org/10.1016/j.isci.2024.111392

SUMMARY

Disulfide bond (Dsb) oxidoreductases involved in oxidative protein folding govern bacterial survival and virulence. Over the past decade, oligomerization has emerged as a potential factor that dictates oxidoreductase activities. To investigate the role of oligomerization, we studied three Dsb-like ScsC oxidoreductases involved in copper resistance: the monomeric *Salmonella enterica* StScsC, and the trimeric *Proteus mirabilis* PmScsC and *Caulobacter crescentus* CcScsC. For copper sequestration, ScsC proteins must remain in the reduced form. However, all three ScsC proteins exhibit both dithiol oxidation and disulfide reduction activity, despite structural differences and previously reported limited *in vitro* activity. Most ScsC reductase activity relies on interactions with *E. coli* DsbD reductase, while oxidase activity depends on environmental oxidation. Interestingly, engineered monomeric PmScsC interacts effectively with the *E. coli* DsbB oxidase, at the partial expense of its reductase activity. These findings highlight oligomerization of oxidoreductases as a steric hindrance strategy to block undesirable upstream oxidative interactions.

INTRODUCTION

Intramolecular disulfide bonds (Dsb) between cysteine (Cys) residues play a central role in the function and stability of many secreted and membrane proteins in both eukaryotes and prokaryotes.[1] In gram-negative bacteria, oxidative protein folding takes place in the periplasmic space and is catalyzed by a group of redox-active disulfide bond (Dsb) proteins characterized by a conserved Cys-X-X-Cys active site.[2,3] The *Escherichia coli* K-12 oxidative protein folding machinery includes four Dsb proteins organized in two distinct redox pathways: the DsbA/DsbB oxidative pathway that introduces disulfide bonds between Cys residues in substrate proteins and the DsbC/DsbD and DsbG/DsbD isomerase pathways that rearranges incorrect disulfide bonds introduced in substrate proteins.[4–6] In this system, the oxidase DsbA enzyme is monomeric,[7] whereas the isomerases DsbC (or DsbG)[8,9] are dimeric, with their catalytic motifs kept in the functionally active oxidized and reduced states, respectively, by specific interactions with the cognate inner membrane oxidase DsbB and reductase DsbD, respectively. While early studies on Dsb proteins have offered a detailed mechanistic understanding of the classical pathways in *E. coli* K-12,[6,7,10–15] much remains to be understood about the diversity in disulfide bond formation systems across other bacteria.[2] It is now established that different bacteria can employ distinct Dsb machineries and encode, in addition to the classical DsbA/B and DsbC/D systems, multiple diverse periplasmic thiol/disulfide oxidoreductases.[2,3,16] One such example is the suppressor of copper sensitivity (Scs) proteins.[17]

Scs proteins were initially discovered as the encoded products of a gene cluster associated with copper tolerance in *Salmonella enterica* serovar Typhimurium.[17] The gene cluster encodes four proteins, ScsA, ScsB, ScsC, and ScsD. A putative copper-binding site and a thioredoxin-like motif containing the catalytic Cys-X-X-Cys site characteristic of Dsb proteins are present in most Scs proteins characterized to date.[17–22] Limited information on the biological function of inner-membrane-associated proteins ScsA and ScsD suggested a role in *S.* Typhimurium periplasmic resistance to H_2O_2 and copper.[23] In comparison, the membrane-bound ScsB protein and soluble periplasmic ScsC protein have been characterized in three *Enterobacteriaceae* species to date: *S.* Typhimurium, *Proteus mirabilis*, and *Caulobacter crescentus*.[18–22] ScsB and ScsC constitute a redox pair that is functionally reminiscent of the *E. coli* DsbC and DsbD system,[18–22] in that ScsB catalytically reduces ScsC *in vivo*.[20,21] *In vitro* evidence suggests ScsC scavenges toxic copper in the cells and delivers it to the copper-binding metallochaperone CueP, thereby reducing cellular toxicity in *S.* Typhimurium.[18,19,22]

On the other hand, crystal structures of the ScsC homologs from *P. mirabilis* (PmScsC) and *C. crescentus* (CcScsC) revealed that their N-terminal regions oligomerize to form strikingly similar

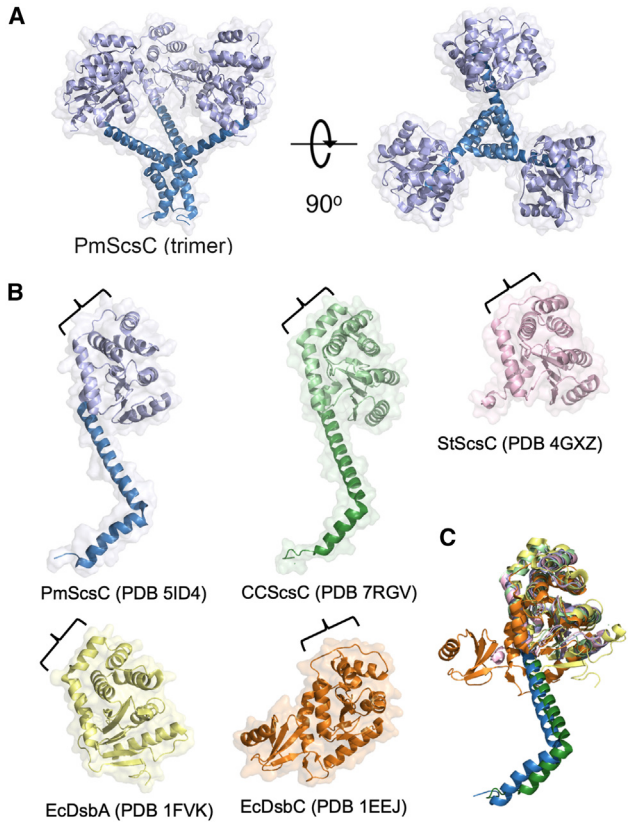

Figure 1. Structural similarity between ScsC homologs and DsbA

(A) The trimeric architecture of PmScsC protein, PDB: 5id4.[20] Trimerization and catalytic domains are displayed in blue and slate, respectively.

(B) Protomer structures of PmScsC (blue/slate: PDB: 5id4 [20]), CcScsC (green: PDB: 7rgv,[18] this protein is a biological trimer), StScsC (pink; PDB: 4gxz,[19] monomeric), EcDsbA (yellow; PDB: 1fvk,[25] monomeric), and EcDsbC (brown; PDB: 1eej,[8] this protein is a biological dimer). The α-helix/loop differences in the globular domains are indicated with a bracket.

(C) Structural superposition of PmScsC, CcScsC, StScsC, and EcDsbA using the secondary-structure matching (SSM) tool from Coot[26] which revealed r.m.s.d. values of 2.9 Å (139 Cα aligned, sequence identity (S.I.) 15%), 2.9 Å (126 Cα aligned, S.I. 17%), and 2.8 Å (143 Cα aligned, S.I. 14%), respectively. This structural superposition showcases that ScsC proteins largely resemble the *E. coli* EcDsbA counterpart, particularly in the TRX domains, despite the overall very low sequence conservation (S.I. 14–17%). EcDsbC aligned structurally to EcDsbA to a certain extent but very poorly aligned to the three ScsC proteins.

trimeric arrangements (Figures 1A and 1B).[18,20] Nonetheless, the catalytic domains in each ScsC protomer resemble that of monomeric *E. coli* DsbA[7] (Figures 1B and 1C). StScsC and CcScsC proteins were reported to function in their reduced state.[21,24] Specifically, the reduced thiols at the catalytic site of StScsC were directly implicated in copper-binding,[22] with no significant disulfide isomerase (or oxidase) activity observed for this homolog *in vitro*.[19,22] Conversely, the trimeric PmScsC and CcScsC proteins had disulfide isomerase activity and lacked dithiol oxidase activity.[20,21]

Considerable progress has been made over the past decades in the genetics, mechanism, and structural understanding of thiol-disulfide oxidoreductases. Aside from redox potential serving an important role in determining specific thiol oxidoreductase catalytic activity, collective evidence from individual studies suggests protein oligomerization also constitutes an important parameter. For example, globular periplasmic monomeric oxidoreductases like EcDsbA are dithiol oxidases, whereas the V-shaped periplasmic homodimeric Dsb proteins EcDsbC and EcDsbG exhibit disulfide isomerase activity.[9,10,27–29] Furthermore, when EcDsbC was engineered to be monomeric, it acquired oxidase activity at the cost of its original disulfide isomerase activity.[30,31] Conversely, when EcDsbA was dimerized, the protein gained disulfide isomerase activity, while its oxidase activity was impacted.[32]

The three structurally characterized ScsC proteins, StScsC, CcScsC, and PmScsC, adopt distinct oligomeric states and exhibit distinct oxidoreductase activities *in vitro*, despite their catalytic domains sharing a striking structural resemblance with monomeric EcDsbA (Figure 1).[18–22] Interestingly, the trimeric PmScsC shared a highly similar globular module and shared the same NCPYC active site with monomeric StScsC, while CcScsC is significantly lower in sequence similarity and uses a rather different active site (RCGYC). Similar to other Dsb proteins, upon the loss of the N-terminal trimeric module, monomerized PmScsC protein (PmScsCΔN) was reported to lose disulfide reductase activity and gain dithiol oxidase activity *in vitro*.[20] Here, we set out to investigate in a cellular context how the quaternary arrangement of thioredoxin-like oxidoreductases influences ScsC function. We used the set of three previously described ScsC homologs (monomeric StScsC and trimeric PmScsC and CcScsC) and the shared genetic background of the model organism *E. coli* K-12.

Herein, we report that all three ScsC proteins possess both dithiol oxidase and disulfide reductase cellular activity, irrespective of their oligomeric state (monomeric or trimeric). Intriguingly, both StScsC and CcScsC but not PmScsC required the EcDsbD electron donor for effective reductase activity in *E. coli* K-12 in the absence of a cognate ScsB partner. Contrastingly, dithiol oxidase activity of ScsC proteins was restricted by the lack of a compatible redox partner in *E. coli* K-12 and was only observed *in vivo* under conditions of environmental oxidation. An engineered monomeric form of PmScsC was the exception, as it could use EcDsbB (the partner of EcDsbA) to efficiently catalyze dithiol oxidation in cells. This study systematically explored the contribution of protein oligomerization in ScsC cellular activity, revealing that it could serve as one strategy by which bacteria can limit redox protein-protein interactions in the cell to maintain oxidoreductase activities that are compatible with the diverse Dsb systems they encode.

RESULTS

ScsC homologs can restore the loss of disulfide oxidase and isomerase pathways in *E. coli*

To assess the different ScsC homologs for disulfide isomerase activity *in vivo* we employed an established *E. coli* assay that monitors colanic acid production.[33] The previously described *E. coli* K-12 strain MC4100 Δ*dsbC* Δ*mdoG* (PL263)[33] was transformed with pSU2718-based expression plasmids containing *scsC* genes from *S.* Typhimurium, *P. mirabilis*, and *C. crescentus* or Ec*dsbC* as the positive control. For strain and plasmid information, see Tables 1 and 2. The deletion of *mdoG* in this *E. coli* strain triggers

Table 1. Bacterial strains used in this study

Strain ID	Strain description	Reference
JCB816	*E. coli* MC1000 *phoR zig12::Tn10* (*malF-lacZ102*)	Bardwell et al.[6]
JCB817	JCB816 Δ*dsbA::kan*	Bardwell et al.[13]
BL21(DE3)	*E. coli* F^- *ompT hsdSB* (rB^- mB^-) *gal dcm* (DE3)	Studier et al.[51]
MT2258	*E. coli* MG1655 Δ*wcaJ::cat*	This work
MT2404	JCB817 with pSU2718-EcDsbA	This work
MT2645	JCB817 with pSU2718-EcDsbC	This work
MT2408	JCB817 with pSU2718-StScsC	This work
MT2405	JCB817 with pSU2718-CcScsC	This work
MT2406	JCB817 with pSU2718-PmScsC	This work
MT2407	JCB817 with pSU2718-PmScsCΔN	This work
MT2644	JCB817 with pSU2718-PmScsC-EcDsbA	This work
MT2409	JCB817 with pSU2718	This work
MT2509	JCB817 with pWSK29-AssT and pSU2718-EcDsbA	This work
MT2659	JCB817 with pWSK29-AssT and pSU2718-EcDsbC	This work
MT2513	JCB817 with pWSK29-AssT and pSU2718-StScsC	This work
MT2510	JCB817 with pWSK29-AssT and pSU2718-CcScsC	This work
MT2511	JCB817 with pWSK29-AssT and pSU2718-PmScsC	This work
MT2512	JCB817 with pWSK29-AssT and pSU2718	This work
JCB818	JCB816 Δ*dsbA::kan1* Δ*dsbB::kan2*	Bardwell et al.[13]
MT2517	JCB818 with pSU2718-EcDsbA	This work
MT2519	JCB818 with pSU2718-StScsC	This work
MT2520	JCB818 with pSU2718-CcScsC	This work
MT2521	JCB818 with pSU2718-PmScsC	This work
MT2522	JCB818 with pSU2718-PmScsCΔN	This work
MT2713	JCB818 with pSU2718-PmScsC-EcDsbA	This work
MT2518	JCB818 with pSU2718	This work
MT2715	JCB818 with pSU2718-PmscsCΔN and pWSK29-EcDsbB	This work
MT2714	JCB818 with pSU2718-PmscsCΔN and pWSK29	This work
PL263	*E. coli* MC4100 Δ*dsbC* Δ*mdoG::kan*	Leverrier et al.[33]
MT1757	PL263 with pSU2718-EcDsbC	This work
MT2682	PL263 with pSU2718-EcDsbA	This work
MT1755	PL263 with pSU2718-StScsC	This work
MT2601	PL263 with pSU2718-CcScsC	This work
MT1706	PL263 with pSU2718-PmScsC	This work
MT2625	PL263 with pSU2718-PmScsCΔN	This work
MT2647	PL263 with pSU2718-PmScsC-EcDsbA	This work
MT1705	PL263 with pSU2718	This work
MT1799	PL263 Δ*mdoG::FRT* Δ*dsbD::FRT*	This work
MT1809	MT1799 with pSU2718-EcDsbC	This work
MT1813	MT1799 with pSU2718-StScsC	This work
MT2602	MT1779 with pSU2718-CcScsC	This work
MT1811	MT1799 with pSU2718-PmScsC	This work
MT1807	MT1799 with pSU2718	This work
MT3760	PL263 with pWSK29	This work
MT3759	PL263 with pWSK29-EcDsbC	This work
MT3757	PL263 Δ*rcsF::cat*	This work
MT3758	MT3757 with pWSK29-EcDsbC	This work

Table 2. Plasmids used in this study

Plasmid ID	Description	Reference
pSU2718	p15A-derived plasmids carry *lacZ*α reporter gene, chloramphenicol resistance	Martinez et al.[52]
pWSK29	pSC101-derived plasmids carry *lacZ*α reporter gene, ampicillin resistance	Wang et al.[53]
pSC108	*C. crescentus scsC* gene with *E. coli dsbA* signal sequence cloned into pDSW204	Cho et al.[21]
pKD3	FRT-flanked cat gene, oriRγ replicon, ampicillin, and chloramphenicol resistance	Datsenko et al.[54]
pKD46	λ recombineering genes (α, β, γ) controlled by arabinose inducible promoter, P*araB*, temperature-sensitive oriR101 replicon, ampicillin resistance	Datsenko et al.[54]
pCP20	*flp* recombinase gene, temperature-sensitive replicon, ampicillin, and chloramphenicol resistance	Cherepanov et al.[55]
pSU2718-EcDsbC	*E. coli dsbC* gene cloned into the BamHI/PstI restriction sites of pSU2718	This work
pSU2718-EcDsbA	*E. coli dsbA* gene cloned into the KpnI/PstI restriction sites of pSU2718	This work
pSU2718-StScsC	*S. enterica scsC* gene cloned into the BamHI/PstI restriction sites of pSU2718	This work
pSU2718-CcScsC	*C. crecentus scsC* gene with DsbA signal sequence cloned into the BamHI/HindIII restriction sites of pSU2718	This work
pSU2718-PmScsC	*P. mirabilis scsC* gene cloned into pSU2718	Furlong et al.[20]
pSU2718-PmScsCΔN	*P. mirabilis scsCΔN* gene with DsbA signal sequence cloned into pSU2718	Furlong et al.[20]
pSU2718-PmScsC-EcDsbA	Pm*scsC*-Ec*dsbA* chimera with DsbA signal sequence cloned into the BamHI/HindIII sites of pSU2718	This work
pWSK29-EcDsbB	*E. coli* MG1655 *dsbB* gene cloned into the EcoRI/HindIII sites of pWSK29	This work
pWSK29-ASST	*assT* gene from *E. coli* CFT073 cloned into the KpnI/PstI sites of pWSK29	This work
pWSK29-EcDsbC	*E. coli dsbC* gene cloned into the BamHI/PstI restriction sites of pWSK29-EcDsbC	This work
pWSK29-StScsC	*S. enterica scsC* gene cloned into pWSK29	Shepherd et al.[19]
pMCSG7	Ligation-independent cloning vector with N-terminal His-tag followed by Tev protease cleavage site incorporated into the leader sequence	Stols et al.[56]
pMCSG7*: *bcfH*	*S. enterica* BcfH mature form (residues 28–281) in pMCSG7	Subedi et al.[22]
pMCSG7*:PmScsC-EcDsbA	Matured Pm*scsC*-Ec*dsbA* chimera in pMCSG7	This work
pLicA:*dsbA*	DsbA mature form in pLicA	Jarrott et al.[57]

cell envelope stress to activate colanic acid biosynthesis that leads to a visually distinctive mucoidal colony morphology on agar plates.[34,35] The outer membrane RcsF protein contains two pairs of disulfide bonds formed between non-consecutive Cys residues. Correct RcsF folding by an active disulfide isomerase, such as EcDsbC is required for subsequent activation of the Rcs signaling cascade, was suggested to account for the mucoidal pattern.[33] We confirmed this being the case, as introducing *rcsF* null mutation completely abolished colanic acid production in MC4100 Δ*dsbC* Δ*mdoG* expressing a plasmid-borne EcDsbC (Figure 2A).

MC4100 Δ*dsbC* Δ*mdoG* strains containing *scsC* expression plasmids were assessed for colanic acid production on minimal M9 media (Figure 2B). Colanic acid biosynthesis (resulting in mucoid colony appearance) was restored in the presence of the native isomerase EcDsbC (positive control strain MC4100 Δ*dsbC* Δ*mdoG*/pEc*dsbC*) but not by EcDsbA (negative control), as expected[33] (Figure 2B). Expression of CcScsC also complemented the disulfide isomerase activity defect in MC4100 Δ*dsbC* Δ*mdoG* (Figure 2B), consistent with a previous report by Cho et al.[21] Complementation with StScsC led to mucoidal colony morphology, evidencing isomerase activity for this protein. The trimeric PmScsC previously reported to possess isomerization activity *in vitro*,[20] was confirmed to function as an isomerase *in vivo* (Figure 2B).

To examine if ScsC proteins have oxidase activity *in vivo*, we employed the *E. coli* swimming motility assay, as introduction of disulfide bonds in FlgI is required for swimming motility in *E. coli*.[36,37] FlgI is a component of the *E. coli* flagellum motility structure that contains an intramolecular disulfide bond catalyzed by EcDsbA. The non-motile JCB816 Δ*dsbA* strain was transformed with *scsC* expression plasmids and compared to EcDsbA and EcDsbC for the restoration of swimming motility. The ScsC expressing strains grew at a similar pattern to EcDsbA in LB (supplemental information, Figure S1), supporting our use of kinetic OD_{600}-based migration assay in this work.[38]

All ScsC proteins partially restored motility in the *dsbA* null strain (Figure 2C), while the EcDsbC control remained immotile. These findings were confirmed in a separate assay that monitors *in vivo* oxidative folding of a different established DsbA substrate, the periplasmic enzyme arylsulfate sulfotransferase (ASST), which catalyzes sulfuryl transfer from a phenolic sulfate to a phenol.[39] ASST contains a disulfide bond required for biochemical activity[40] and is found in several bacterial species, including uropathogenic *E. coli*.[41,42] A plasmid containing the *assT* gene (pASST) was transformed into the same set of

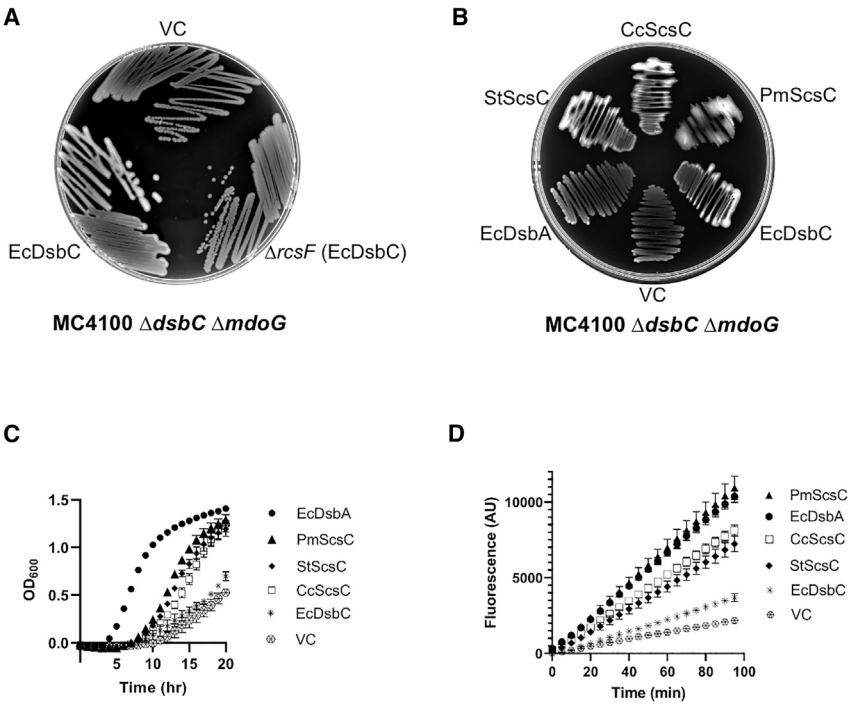

Figure 2. ScsC proteins display both disulfide isomerase and oxidase activity in *E. coli*

(A) Mucoidal colony morphology in *mdoG* null mutant is RcsF-dependent (VC is vector control, pWSK29).

(B) Complementation of RcsF folding and restoration of mucoidal colony morphology in strain MC4100 Δ*dsbC* Δ*mdoG* by disulfide isomerase EcDsbC (positive control), ScsC proteins, or EcDsbA (negative control) expressed from the same plasmid vector (VC, pSU2718). The plate image (representative of three independent repeats) shows complemented strains grown on solid M9 minimal media following incubation at 29°C for 48 h.

(C) Complementation of FlgI folding and restoration of flagella-mediated swimming motility in strain JCB816 Δ*dsbA* by EcDsbA, ScsC proteins, EcDsbC (negative control), or empty VC (pSU2718). Strain motility zones on semi-solid LB media were measured as optical density (OD_{600nm}) every 5 min over 20 h of continuous incubation at 37°C.

(D) Complementation of ASST folding and restoration of cellular sulfotransferase activity in strain JCB816 Δ*dsbA* pAssT by EcDsbA, ScsC proteins, EcDsbC (negative control), or empty VC (pSU2718). ASST activity was monitored by fluorogenic substrate intensity measured every 5 min over 95 min; Data in panels C and D show mean values derived from biological triplicates with error bars representing the standard deviation (SD).

E. coli JCB816 Δ*dsbA* strains used in the motility assays, and ASST oxidative folding by ScsC proteins was compared to the EcDsbA positive control. While the expression of EcDsbC leads to a very weak ASST activity that closely resembles the vector control in the *dsbA* null mutant, the ASST activity of strains encoding ScsC homologs was comparable or slightly reduced levels to EcDsbA, confirming ScsC oxidase activity *in vivo* (Figure 2D). Collectively, these results demonstrate that despite previous reports of ScsC enzymes acting predominantly as isomerases *in vitro*, *in vivo* they can act both as isomerases and oxidases and participate in mainstream oxidative protein folding pathways present in *E. coli* K-12.

DsbD but not DsbB serves as a heterologous redox partner for ScsC in *E. coli*

To further investigate the participation of ScsC proteins in *E. coli* oxidative protein folding pathways, we examined if *in vivo* ScsC activity required DsbB and DsbD, which are the respective redox partners of DsbA and DsbC in *E. coli*. Interestingly, deletion of *dsbB* in the *E. coli* strains assessed for swimming motility on rich media did not alter the original strain phenotype, indicating that ScsC expression could alone restore *E. coli* motility in the absence of EcDsbA and EcDsbB under these conditions (Figures 3A and 3B). This was, however, also observed with EcDsbA, which under the test conditions, could fully complement motility despite loss of EcDsbB (Figures 3A and 3B). Full restoration of motility in a Δ*dsbB* strain was previously reported to occur with exogenously supplemented oxidants[36] presumably through environmental oxidation of EcDsbA. For this reason, we repeated motility assays in minimal M9 media. Note that the strains grew significantly slower in M9 compared to LB (supplemental information, Figure S2), and in this case, tracking migration across minimal media agar surface was significantly affected by various confounding factors including lid condensation. We thus opted to use the qualitative assessment of migration on agar surface for all motility experiments conducted in minimal media.

Under the test conditions in minimal media, strains remained immotile (Figure 3C), confirming that environmental oxidation of EcDsbA, as well as of ScsC proteins, was responsible for the motility restoration observed in rich media. In contrast, in minimal media, the motility of the JCB816 Δ*dsbA* (DsbB+) strain was only fully restored by complementation with EcDsbA, while ScsC expressing strains remained immotile, except the strain expressing PmScsC showed marginal complementation of motility under the test conditions (Figure 3D). However, this lack of motility in JCB826 Δ*dsbA* is reversed in an ScsC-dependent manner when the minimal media is supplemented with a strong exogenous oxidant, cystine (Figure 3D). We conclude that ScsC proteins can be active as oxidases in *E. coli* K-12 and fold different DsbA substrates but only under oxidant supplementation conditions, as their oxidase activity is not maintained by DsbB *in vivo*.

The lack of DsbB dependency for oxidase activity by the ScsC proteins *in vivo* prompted us to investigate their requirement for DsbD as a redox partner for isomerase activity next. For this, we constructed a *dsbD* null mutation in MC4100 Δ*dsbC* Δ*mdoG*, the reporter strain for isomerase activity. When the Δ*dsbC* Δ*mdoG* knockout strain was complemented with EcDsbC alone, the hallmark mucoidal morphology induced by RcsF folding was observed (Figure 4A). This mucoidal morphology was reduced in the MC4100 Δ*mdoG* Δ*dsbD* Δ*dsbC* strain confirming DsbC

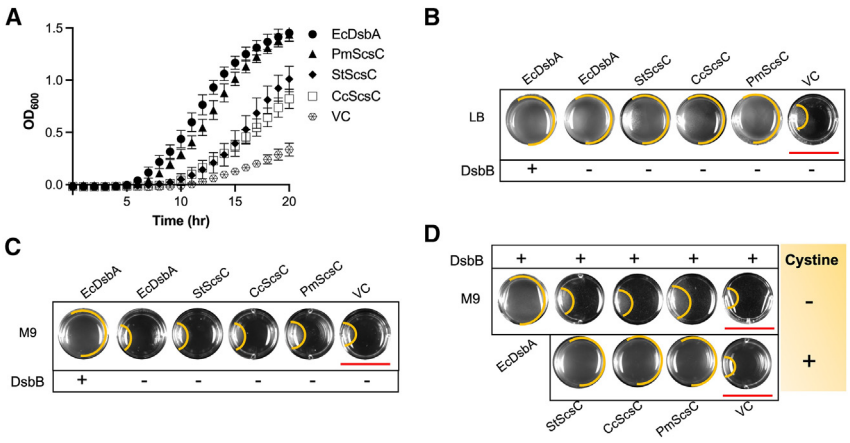

Figure 3. Dithiol oxidase activity of ScsC proteins in *E. coli* is dependent on exogenous oxidants

(A and B) Expression of EcDsbA and ScsC proteins but not empty vector control (VC, pSU2718) restore swimming motility in JCB816 Δ*dsbA* Δ*dsbB* in rich media (panel A shows motility kinetics monitored by OD_{600} measured every 5 min over 20 h and panel B shows motility plate image taken at 20 h with swimming zone edge marked in yellow).

(C) Expression of ScsC proteins does not restore swimming motility in JCB816 Δ*dsbA* Δ*dsbB* in minimal media (plate image taken at 20 h).

(D) Expression of EcDsbA but not ScsC proteins fully restores swimming motility in JCB816 Δ*dsbA* (DsbB+) in minimal media without exogenous oxidant (plate image taken at 20 h). For experiments that required the addition of an exogenous oxidant, cystine (100 μM) similar to the level found in LB was added. Data plotted in A are mean values from biological triplicates with SD values shown as error bars. Scale bars (red) in panels B, C, and D, 12 mm. The images shown in panels B–D are representative of at least three independent replicates.

dependence on DsbD for isomerase activity. Similarly, expression of StScsC and CcScsC in a strain lacking DsbD and DsbC showed reduced colanic acid production compared to an isogenic strain with DsbD (Figure 4B). In contrast, strains expressing PmScsC retained high colanic acid production irrespective of DsbD presence or absence (Figures 4A and 4B). This is supported by the redox state of PmScsC, which was shown to be primarily reduced in $DsbD^+$ or $DsbD^-$ strains using AMS alkylation and western blot analysis (Figure 4C). This PmScsC was confirmed to be located in the periplasmic space using extracted periplasmic fractions, while the oxidation state determined from AMS alkylation remained consistent to that of the whole cell extract (Figure 4D). These results suggest that, like EcDsbC, efficient disulfide isomerase activity by StScsC and CcScsC, but not by PmScsC, in *E. coli* requires DsbD.

Monomeric PmScsC requires DsbB to function as a dithiol oxidase in *E. coli*

The intriguing activity of PmScsC as an efficient DsbD-independent isomerase, combined with its capacity to fold DsbA substrates upon becoming environmentally oxidized, prompted us to investigate this intriguing disulfide catalyst further. The PmScsC quaternary structure consists of three protomers that are tethered together into a trimer (Figure 1).[20] Trimerization occurs through the oligomerization of a modular N-terminal trimerization domain.[20] Full-length PmScsC failed to oxidize dithiol peptides *in vitro*,[20] but upon removing the trimerization domain (PmScsCΔN) the protein adopted a monomeric structure (confirmed by size exclusion chromatography and multiangle laser light scattering) that acquired oxidase activity at the expense of isomerase activity *in vitro*.[20,43] We hypothesized that monomeric PmScsCΔN also attains the ability to interact with EcDsbB and function as an efficient oxidase in *E. coli*. To test this, we compared motility restoration in strain JCB816 Δ*dsbA* by PmScsC and PmScsCΔN in minimal media. Under these conditions, only the monomeric PmScsCΔN restored bacterial motility to EcDsbA levels (Figure 5A). Motility restoration by PmScsCΔN was dependent on DsbB, similar to EcDsbA, as the expression of PmScsCΔN in JCB816 Δ*dsbA* Δ*dsbB* failed to restore bacterial motility, unless the strain was complemented with a plasmid expressing EcDsbB (Figure 5B). Consistent with the gain in dithiol oxidase activity, the isomerase activity of PmScsCΔN is significantly reduced in contrast to trimeric PmScsC in *E. coli* (Figures 5C and 5D).

To further explore the activity of PmScsC in the native trimer and monomer form, we modeled the interaction of PmScsC and PmScsCΔN with EcDsbB. *In silico* analyses revealed that in the trimer form, PmScsC can only interact with DsbB in the compact configuration (one of three conformations adopted by PmScsC), and only using one of the catalytic sites (Figure 6A). In contrast, the monomer PmScsCΔN can form a complex with EcDsbB that is similar to the structurally solved EcDsbA-EcDsbB complex (Figures 6B–6D). Together, our results confirm that monomeric (PmScsCΔN), but not trimeric PmScsC is an effective thiol oxidase that forms a functional redox pair with DsbB catalyzing oxidative protein folding in the *E. coli* periplasm.

Trimeric EcDsbA retains disulfide oxidase activity without gain of isomerase activity in *E. coli*

The change of catalytic activity observed in PmScsC from a disulfide isomerase to an oxidase purely by altering its oligomeric state, prompted us to investigate whether modulation of catalytic activity could be engineered into the prototypical monomeric *E. coli* thiol oxidase DsbA by oligomerization. For this, we constructed a PmScsC-EcDsbA chimeric protein that consists of the modular N-terminal PmScsC linker domain preceding the mature EcDsbA sequence. Over-expression of PmScsC-EcDsbA was carried out in BL21(DE3) and purified to homogeneity using IMAC, followed by TEV cleavage, reverse IMAC and size exclusion chromatography (SEC) (Figure 7A). The secondary structure of PmScsC-EcDsbA in both oxidized and reduced state was assessed by CD spectroscopy, which showed a predominantly α-helical secondary structure as reflected by the double minima at 208 and 222 nm, which is expected for folded DsbA-like proteins (Figure 7B). The trimeric oligomerization state in a solution of the PmScsC-EcDsbA chimera was analyzed by size

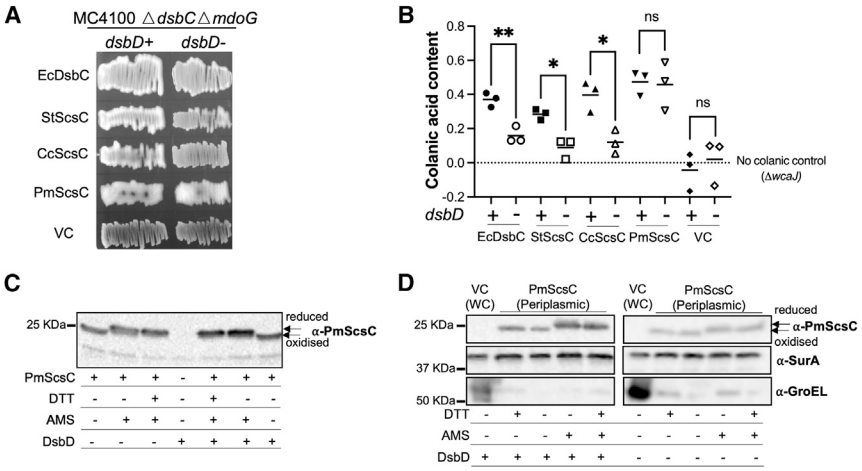

Figure 4. Requirement for DsbD in maintaining ScsC disulfide isomerase activity in *E. coli*

(A) Restoration of RcsF-dependent colanic acid production and mucoidal colony morphology in strains MC4100 Δ*mdoG* Δ*dsbC* (left) and MC4100 Δ*mdoG* Δ*dsbC* Δ*dsbD* (right) by EcDsbC and ScsC proteins expressed from the same plasmid vector pSU2718, or empty vector control (VC). The plate image shows complemented strains grown on solid minimal media following incubation at 29°C for 48 h (the plate image represents at least three biological replicates).

(B) Quantitation of colanic acid content (data derived from three biological replicates); (C) AMS alkylation of free cysteine residues in PmScsC proteins prepared from whole cell (WC) samples of MC4100 Δ*dsbC* Δ*mdoG* in DsbD- and DsbD+ backgrounds (VC control was included to show the specificity of α-PmScsC antibody).

(D) AMS alkylation of free cysteine residues in PmScsC proteins prepared from extracted periplasmic subcellular fractionation (VC derived from WC samples was used as the subcellular fractionation control). Welch's t test was used in panel B, p = 0.01–0.05 (*), p =0.001–0.01 (**), ns is the abbreviation for no significance. α-SurA (periplasmic specific) and α-GroEL (cytosolic specific) antibodies were used to assess the quality of the periplasmic extracts used in panel D.

exclusion chromatography (SEC) and sedimentation velocity analytical ultracentrifugation (SV-AUC). SEC analysis showed that PmScsC-EcDsbA elutes at a similar elution volume as previously described trimeric DsbA-like proteins (PmScsC [molecular weight 74.3 kDa[20]] and BcfH [molecular weight 82.8 kDa,[22]]) and earlier than monomeric EcDsbA (23.1 kDa), suggesting that the chimera oligomerizes in solution (Figure 7C). SV-AUC analysis was performed to confirm the molecular weight of PmScsC-EcDsbA. The results indicate that this chimera has a molecular weight of 79 kDa (Figure 7D), approximately 3-times the molecular weight of monomeric PmScsC-EcDsbA (27 kDa) and consistent with the formation of a trimer. To further validate this *in vivo*, we isolated periplasmic fractions from strains expressing PmScsC-EcDsbA and performed western blot analysis using an anti-EcDsbA antibody. Despite the disruptive effects of the isolation procedures, we observed a band just above 75 kDa, consistent with the trimeric form of the protein, particularly when SDS detergent concentrations in the sample buffer were reduced (supplemental information, Figure S3). Altogether, these results indicate that the addition of the N-terminal trimerization of EcDsbA resulted in a trimeric PmScsC-EcDsbA chimera.

To assess the activity of trimeric EcDsbA *in vivo*, we expressed the PmScsC-EcDsbA chimera in *E. coli* and assessed its capacity to restore swimming motility and colanic acid production in relevant strains (Figure 8A). Surprisingly, full motility restoration of strain JCB816 Δ*dsbA* was mediated by the trimeric DsbA chimera, at similar levels to wild-type monomeric EcDsbA (positive control) (Figures 8B and 8C). Like monomeric EcDsbA, the trimeric protein failed to restore colanic acid production in MC4100 Δ*dsbC* Δ*mdoG* (Figures 8D and 8E). Collectively our findings demonstrate that trimerization of EcDsbA does not affect its strong thiol oxidation activity or impart it with an additional isomerization function in the cell.

DISCUSSION

Disulfide bond catalysis by bacterial Dsb proteins governs the oxidative folding of several extra-cytoplasmic proteins in the periplasmic space.[2,3,16,44] This oxidative protein folding process plays a crucial role in bacterial physiology, survival, antimicrobial resistance, and virulence.[2,3] The redox activities of archetypal Dsb proteins, best characterized in *E. coli* K-12, are typically tied to their oligomerization state, i.e., monomeric and dimeric Dsb proteins, represented by DsbA and DsbC (and DsbG), which catalyze thiol oxidation and disulfide isomerization, respectively.[2,3,16] Much less is known, however, of other periplasmic thiol/disulfide oxidoreductases reported to adopt a variety of oligomeric structures and whether this can predict distinct catalytic activities in the cell remains unknown.[2]

Based on a growing body of evidence,[9,10,20,25,27–31,45] the prevailing model is that the functional fate of a thiol/disulfide oxidoreductase as an oxidase or reductase is primarily governed by its oligomeric state in the bacterial periplasm, with steric hindrance preventing non-functional interactions and keeping oxidative/reductive pathways independent. In this work, we directly investigated this model using a set of previously described ScsC proteins from different bacterial species, studied in the well-characterized genetic background of *E. coli* K-12. The three studied ScsC homologs were previously reported to adopt distinct quaternary architectures, including two recently characterized trimeric ScsC homologs (CcScsC and PmScsC) that are functionally analogous to DsbC *in vitro*, and the monomeric StScsC that lacked disulfide oxidase and isomerase activity.[18–21,43] Here, we demonstrated that all three ScsC proteins, despite differences in native oligomeric structure, can exhibit dual dithiol oxidase and disulfide isomerase activities *in vivo* under the conditions tested. Our findings may be explained by the natural limitations inherent to *in vitro* assays, in which the parameters may be affected by the artificial assay conditions that deviate from the cellular environment.[18–21,43] The latter highlights the importance of confirming enzyme function *in vivo*, in particular for dithiol redox catalysts from diverse systems that co-exist in the same organism.

Bacterial periplasmic oxidoreductases are considerably diverse; while some are inherently housekeeping, others are only found in specific serovars or strains.[2,3] For instance, in addition to the housekeeping EcDsbA/EcDsbB pathway of *E. coli*

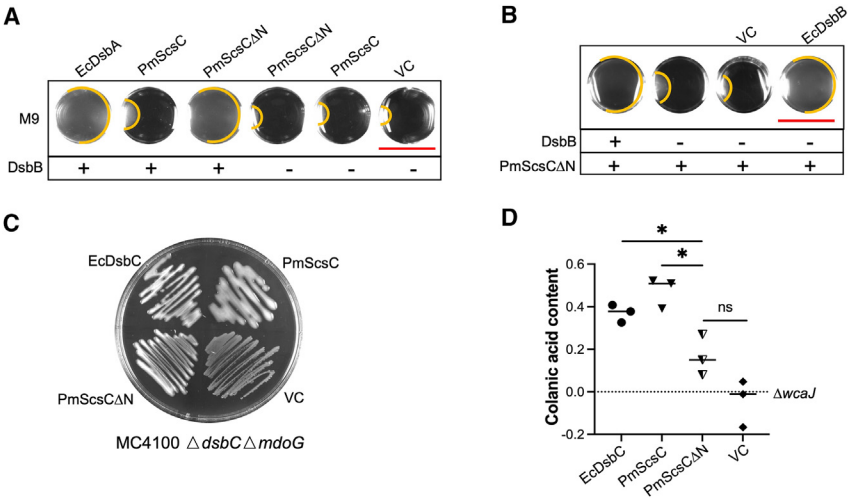

Figure 5. The oligomeric state of PmScsC dictates its disulfide oxidoreductase activity and redox protein interactions in *E. coli*

(A) Motility of JCB816 Δ*dsbA* (DsbB+) and JCB816 Δ*dsbA* Δ*dsbB* (DsbB-) upon the expression of EcDsbA (positive control), PmScsC (trimeric) and PmScsCΔN (monomeric) in minimal media.

(B) Restoration of motility in JCB816 Δ*dsbA* Δ*dsbB* (DsbB-) expressing PmScsCΔN required either chromosomal encoded or EcDsbB cloned into pWSK29.

(C) Pattern of RcsF-dependent colanic acid production in strain MC4100 Δ*mdoG* Δ*dsbC* by EcDsbC (positive control), PmScsC (trimeric), PmScsCΔN (monomeric) or empty VC (pSU2718).

(D) Quantitation of colanic acid contents (data derived from three biological replicates). EcDsbC, PmScsC, and VC (pSU2718) colanic acid quantitation in panel D were the same dataset used in Figure 4B. Welch's t test was used in panel D, p = 0.01–0.05 (*), ns is the abbreviation for no significance. Scale bars (red) in panels A and B, 12 mm. All images shown represent at least three independent replicates.

K-12, uropathogenic *E. coli* strains also encode DsbL/DsbI, an extra redox pair that may be dedicated to the oxidative folding of virulence factors.[46] Cho et al.[21] reported the lack of a conventional Dsb reductive pathway in *C. crescentus* that is functionally supplied by CcScsC and CcScsB. However, in *S.* Typhimurium, the StScsC/StScsB pair co-exists with several Dsb oxidative and reductive pathways, and it was thought to exhibit no functional overlap.[19] Interestingly, we report that none of the characterized ScsC proteins can interact with EcDsbB, the cognate oxidase partner of DsbA in the prototypical *E. coli* system. However, consistent with previous biochemical evidence that StScsC and DsbD constitute a redox-relay pair,[24] in our study, both CcScsC and StScsC, required DsbD to reduce disulfides efficiently *in vivo* (Figure 4). Considering that DsbA/B and DsbC/D systems constitute the generic Dsb machinery, this fits the previous observation that reduced StScsC sequesters copper,[24] i.e., reductive interactions with DsbD are, in fact, favorable for ScsC proteins, and explain the homology between ScsB (the cognate redox pair for ScsC) with DsbD, but oxidative reactions would deem detrimental to their capacity to bind copper.[21] Our finding further explained how ScsC proteins stay predominantly in their reduced form in the periplasm to counteract copper and oxidative stress.[19,23,24] Aside from pairing with ScsB/DsbD for redox relay, the ScsC proteins evade interactions with the prototypical Dsb oxidase system.

PmScsC presents an interesting exception. In *E. coli* K-12, PmScsC still functions as an effective disulfide isomerase independently of DsbD (Figure 4) and displays weak dithiol oxidase activity. This observation is supported by the finding that PmScsC is found reduced in the periplasm (Figures 4C and 4D), which would allow isomerase activity, while its oxidation by DsbB is sterically hindered (Figure 6), which would diminish oxidase function in *E. coli* K-12 (Figure 3). How PmScsC is found reduced in the absence of cognate

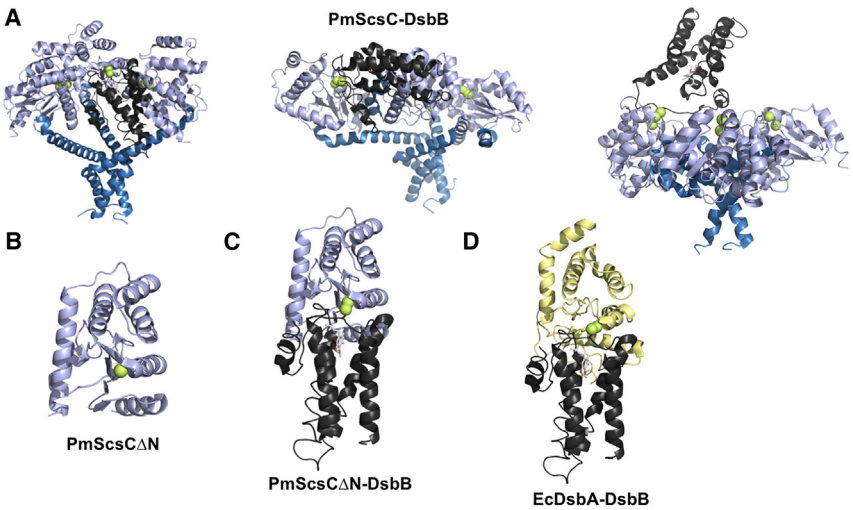

Figure 6. *In silico* analysis of the interaction of EcDsbB (Black) with PmScsC trimer and monomer

(A) PmScsC (purple/blue) adopts three conformations, extended (left), transitional (middle), and compact (right). Modeling of PmScsC interactions with EcDsbB generated by superposition of the catalytic monomer in the trimer with exposed catalytic cysteines with EcDsbA-DsbB complex (PDB: 3E9J)[39] showed that only the compact configuration (right panel) would allow for the catalytic domain to interact with EcDsbB.

(B) Crystal structure of PmScsCΔN (PDB: 6NEN).[20]

(C) Model of the interaction of PmScsCΔN with EcDsbB generated by superposition of PmScsCΔN onto EcDsbA in complex with EcDsbB.

(D) Crystal structure of EcDsbA C32-EcDsbB C104 complex (EcDsbA in yellow). Catalytic cysteines are shown as lemon-colored spheres (left).

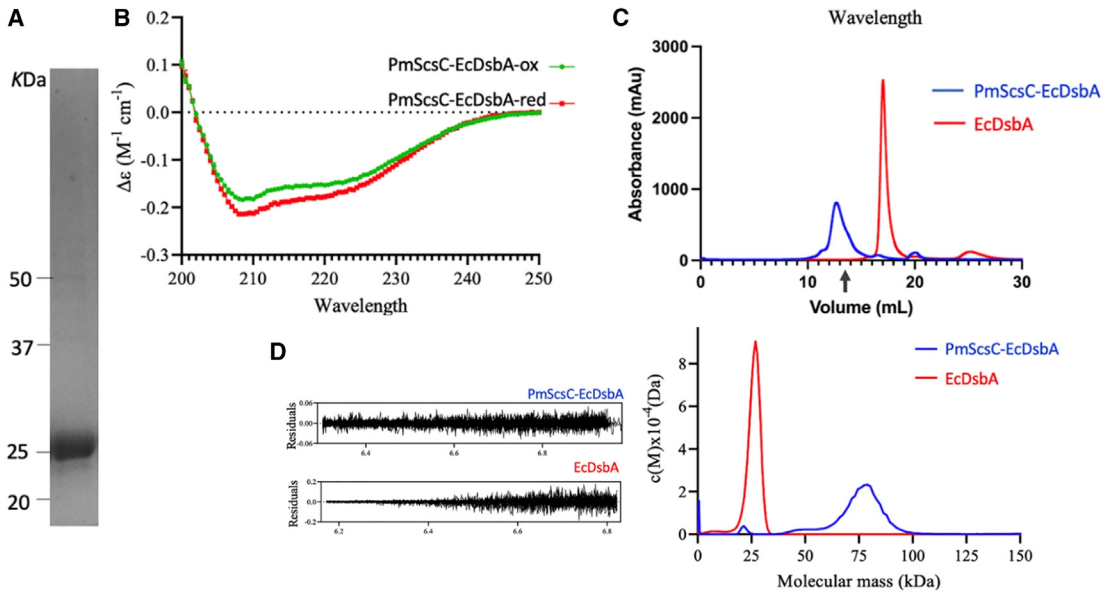

Figure 7. PmScsC-EcDsbA chimera production and biophysical characterization

(A) SDS-PAGE analysis of purified PmScsC-EcDsbA (monomer molecular weight 27 kDa).

(B) Circular dichroism spectra of oxidized and reduced PmScsC-EcDsbA. CD measurements were at 20°C and plotted as molar ellipticity $\Delta\varepsilon$ (M^{-1} cm^{-1}) as a function of the wavelength (200–250 nm).

(C) Size exclusion chromatography elution profiles PmScsC-EcDsbA (blue) and monomeric EcDsbA (red). The black arrow indicates the elution volume previously determined for trimeric DsbA-like proteins, *S. enterica* BcfH and PmScsC.[20,22]

(D) Sedimentation velocity analytical ultracentrifugation analysis displaying the continuous mass [c(M)] distribution as a function of molecular mass (kDa) of PmScsC-EcDsbA and EcDsbA at 2 mg mL^{-1} with residuals for *c*(M) of PmScsC-EcDsbA and EcDsbA displayed previously.

reductase DsbD in *E. coli* K-12, may be explained by pools of reduced PmScsC being generated in the cell after having performed substrate protein oxidation. While less likely, it may also be proposed that, yet unidentified partners can reduce PmScsC in the periplasmic space of *E. coli* K-12. Unlike the full-length PmScsC, the monomeric PmScsCΔN forms an oxidase pair with EcDsbB in *E. coli* and is functionally equivalent to EcDsbA (Figures 5 and 6), at the detriment of its original disulfide reductase activity (Figures 5C and 5D). Thus, the oligomerization of PmScsC is adopted as a strategy to exclude undesirable oxidoreductive interactions, lending support to the steric hindrance model. Bader et al.[31] also showed that a monomeric variant of EcDsbC interacted with DsbB and acquired oxidase activity.[31] Nonetheless, the monomeric StScsC, in pairing with DsbD, demonstrated an efficient isomerase substitute to DsbC (Figures 3 and 4). We conclude that while protein oligomerization may serve as a mechanism to control functional overlap across different disulfide oxidoreductases in certain bacteria, the cellular activities of periplasmic TRX-fold proteins cannot only be inferred by the protein's oligomerization status.

Limitations of the study

This study has several limitations. In this work, EcDsbA was trimerized by engineering the N-terminal domain of PmScsC to the canonical EcDsbA. The resulting chimera protein gives no observable disulfide isomerase activity while retaining oxidase activity *in vivo* under the test conditions. One may explain that the lack of isomerization activity is due to this activity not relying on the trimerization of EcDsbA. Indeed, there is evidence of Dsb-like proteins not following the oligomerization-isomerase rule, in that the monomeric StScsC was shown to be a suitable substrate of DsbD in the isomerization pathway but not DsbB (Figures 3 and 4).[24] However, it is also possible that the engineered EcDsbA units are being placed in unfavorable orientations/positions within the chimera trimer to allow for functional interactions. This aspect will require further detailed investigation to design robust cellular oxidative protein folding biotechnological strategies.

Oligomeric proteins can be quite vulnerable to changes by the addition of protein tags.[47–50] We avoided using heterologous tags to prevent potential changes in protein function or interactions. To address concerns about protein expression levels affecting function, we used genetically similar *E. coli* strains for functional assays and controlled expression conditions with identical promoters, 5′ UTRs, and signal sequences (except StScsC for which the native is used). This standardization aimed to minimize variability in protein levels that may impact the observed functional differences derived from transcriptional and translational initiations.

RESOURCE AVAILABILITY

Lead contact

Further information and requests should be directed and will be fulfilled by the lead contact, Yaoqin Hong (yaoqin.hong@jcu.edu.au).

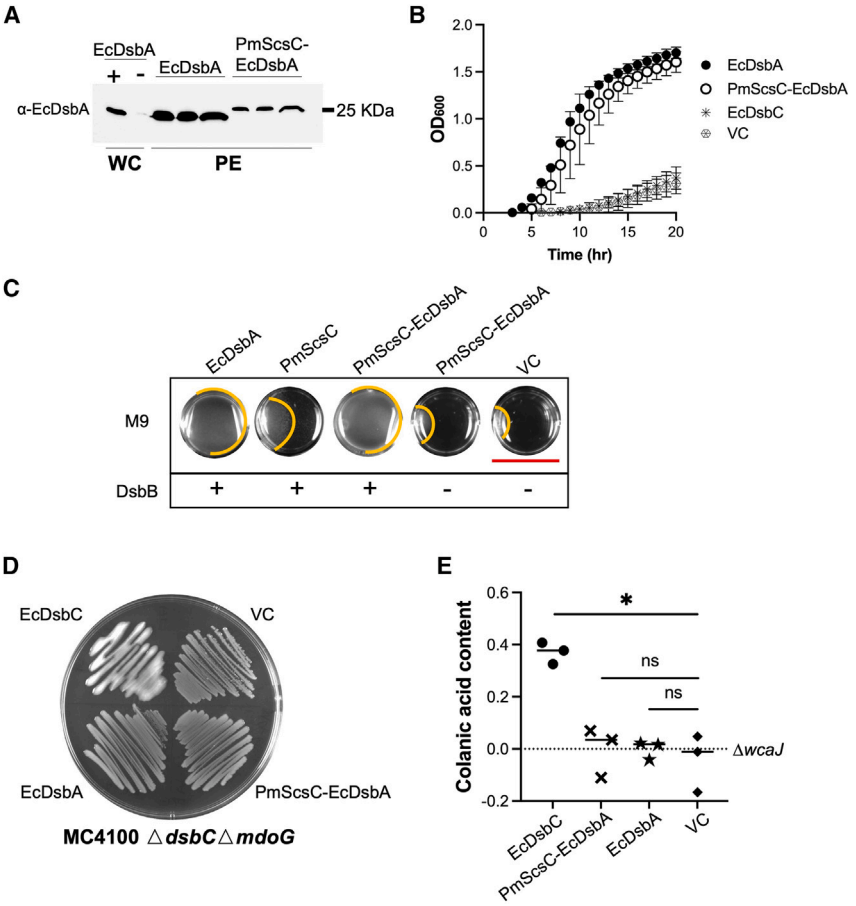

Figure 8. Trimerization of EcDsbA does not affect its disulfide oxidoreductase function in *E. coli*

(A) Localization of full-length mature PmScsC-EcDsbA to the periplasm.

(B) The expression of PmScsC-EcDsbA chimera restores swimming motility of JCB816 Δ*dsbA* in LB.

(C) Restoration of swimming motility in minimal media for strain JCB816 Δ*dsbA* (DsbB+) expressing EcDsbA (monomeric), PmScsC (trimeric) and PmScsC-EcDsbA chimera (trimeric) and isogenic *dsbB* mutant JCB816 Δ*dsbA* Δ*dsbB* (DsbB-) complemented with the PmScsC-EcDsbA chimera or empty VC (pSU2718).

(D) Restoration of RcsF-dependent colanic acid production in strain MC4100 Δ*mdoG* Δ*dsbC* by disulfide isomerase EcDsbC (positive control), EcDsbA (monomeric), PmScsC-EcDsbA chimera (trimeric) or empty VC (pSU2718).

(E) Quantitation of colanic acid contents (data derived from three biological replicates). EcDsbC and VC colanic acid quantitation values in panel E were the same dataset in Figure 4B. Welch's t test was used in panel C, p = 0.01–0.05 (*), ns is the abbreviation for no significance. Scale bars (red) in panel C, 12 mm. All images shown represent at least three independent replicates.

Materials availability

The plasmids and strains generated in this study are available upon request.

Data and code availability

- Data: Original western blot images are supplied in the supplemental information of this study.
- Code: Not applicable to this work.
- All other items: Any additional data required to reanalyze the data reported in this work is available from the lead contact upon request.

ACKNOWLEDGMENTS

This work was supported by an Australian Research Council Discovery Project (DP190101613) to M.T. and B.H.; Clive and Vera Ramaciotti Health Investment Grant (2017HIG0119) to M.T., and a Georgina Sweet Award for Women in Quantitative Biomedical Science to M.T.; The Ian Potter Foundation sponsored CLARIOStar high-performance microplate reader (BMG, Australia). M.T. received support from the Queensland University of Technology through a Vice-Chancellor's Research Fellowship. Y.H. was supported by an Early Career Researcher Award from the Faculty of Health, Queensland University of Technology. We thank Dr Anthony Verderosa for constructing pSU2718-EcDsbA. Vectors pMCSG7:PmscsC and pSC108 (DsbAss-CcScsC) were, respectively, gifted by Professor Jennifer L. Martin (Griffith University, Australia) and Professor Jean-François Collet (Institut de Duve, Universite' Catholique de Louvain, Belgium). The authors thank Professor Jennifer L. Martin for critically reviewing the manuscript and acknowledge the use of the La Trobe University Comprehensive Proteomics Platform.

AUTHOR CONTRIBUTIONS

Y.H.: conceptualization, methodology, formal analysis, investigation, visualization, writing—original and draft, writing—review and editing; J.Q.: investigation, writing—review and editing; L.M.: investigation, formal analysis, visualization; J.J.P.: investigation, methodology, writing—review and editing; B.H.: visualization, supervision, writing—original and draft, writing—review and editing, funding acquisition; M.T.: conceptualization, methodology, supervision, writing—review and editing; funding acquisition. All authors approved the final manuscript.

DECLARATION OF INTERESTS

M.T. is an employee of the GSK group of companies. This research was conducted in the absence of any commercial or financial relationships that could be constructed as a potential conflict of interest.

STAR★METHODS

Detailed methods are provided in the online version of this paper and include the following:

- KEY RESOURCES TABLE
- EXPERIMENTAL MODEL AND STUDY PARTICIPANT DETAILS
- METHOD DETAILS
  - Bacterial genetics methods
  - Swimming motility assay
  - ASST sulfotransferase assay
  - Mucoidal colony morphology assay to track colanic acid production
  - Colanic acid quantification
  - Labelling free cysteines groups, periplasmic extractions, and Western blot

- Purification of PmScsC-EcDsbA chimera
- Protein biophysical characterisation

- QUANTIFICATION AND STATISTICAL ANALYSIS

SUPPLEMENTAL INFORMATION

Supplemental information can be found online at https://doi.org/10.1016/j.isci.2024.111392.

Received: March 28, 2024
Revised: September 24, 2024
Accepted: November 12, 2024
Published: November 15, 2024

REFERENCES

1. Sevier, C.S., and Kaiser, C.A. (2002). Formation and transfer of disulphide bonds in living cells. Nat. Rev. Mol. Cell Biol. *3*, 836–847. https://doi.org/10.1038/nrm954.
2. Heras, B., Shouldice, S.R., Totsika, M., Scanlon, M.J., Schembri, M.A., and Martin, J.L. (2009). DSB proteins and bacterial pathogenicity. Nat. Rev. Microbiol. *7*, 215–225. https://doi.org/10.1038/nrmicro2087.
3. Landeta, C., Boyd, D., and Beckwith, J. (2018). Disulfide bond formation in prokaryotes. Nat. Microbiol. *3*, 270–280. https://doi.org/10.1038/s41564-017-0106-2.
4. Manta, B., Boyd, D., and Berkmen, M. (2019). Disulfide Bond Formation in the Periplasm of Escherichia coli. EcoSal Plus *8*, 10–1128. https://doi.org/10.1128/ecosalplus.ESP-0012-2018.
5. Heras, B., Kurz, M., Shouldice, S.R., and Martin, J.L. (2007). The name's bond, disulfide bond. Curr. Opin. Struct. Biol. *17*, 691–698. https://doi.org/10.1016/j.sbi.2007.08.009.
6. Bardwell, J.C., Lee, J.O., Jander, G., Martin, N., Belin, D., and Beckwith, J. (1993). A pathway for disulfide bond formation *in vivo*. Proc. Natl. Acad. Sci. USA *90*, 1038–1042. https://doi.org/10.1073/pnas.90.3.1038.
7. Martin, J.L., Bardwell, J.C., and Kuriyan, J. (1993). Crystal structure of the DsbA protein required for disulphide bond formation *in vivo*. Nature *365*, 464–468. https://doi.org/10.1038/365464a0.
8. McCarthy, A.A., Haebel, P.W., Törrönen, A., Rybin, V., Baker, E.N., and Metcalf, P. (2000). Crystal structure of the protein disulfide bond isomerase, DsbC, from Escherichia coli. Nat. Struct. Biol. *7*, 196–199. https://doi.org/10.1038/73295.
9. Heras, B., Edeling, M.A., Schirra, H.J., Raina, S., and Martin, J.L. (2004). Crystal structures of the DsbG disulfide isomerase reveal an unstable disulfide. Proc. Natl. Acad. Sci. USA *101*, 8876–8881.
10. Zapun, A., Missiakas, D., Raina, S., and Creighton, T.E. (1995). Structural and Functional Characterization of DsbC, a Protein Involved in Disulfide Bond Formation in Escherichia coli. Biochemistry *34*, 5075–5089. https://doi.org/10.1021/bi00015a019.
11. Inaba, K., Murakami, S., Suzuki, M., Nakagawa, A., Yamashita, E., Okada, K., and Ito, K. (2006). Crystal structure of the DsbB-DsbA complex reveals a mechanism of disulfide bond generation. Cell *127*, 789–801.
12. Missiakas, D., Georgopoulos, C., and Raina, S. (1993). Identification and characterization of the Escherichia coli gene dsbB, whose product is involved in the formation of disulfide bonds *in vivo*. Proc. Natl. Acad. Sci. USA *90*, 7084–7088. https://doi.org/10.1073/pnas.90.15.7084.
13. Bardwell, J.C., Mcgovern, K., and Beckwith, J. (1991). Identification of a Protein Required for Disulfide Bond Formation Invivo. Cell *67*, 581–589. https://doi.org/10.1016/0092-8674(91)90532-4.
14. Stewart, E.J., Katzen, F., and Beckwith, J. (1999). Six conserved cysteines of the membrane protein DsbD are required for the transfer of electrons from the cytoplasm to the periplasm of Escherichia coli. EMBO J. *18*, 5963–5971.
15. Kadokura, H., Tian, H., Zander, T., Bardwell, J.C.A., and Beckwith, J. (2004). Snapshots of DsbA in action: detection of proteins in the process of oxidative folding. Science *303*, 534–537.
16. Shouldice, S.R., Heras, B., Walden, P.M., Totsika, M., Schembri, M.A., and Martin, J.L. (2011). Structure and function of DsbA, a key bacterial oxidative folding catalyst. Antioxidants Redox Signal. *14*, 1729–1760. https://doi.org/10.1089/ars.2010.3344.
17. Gupta, S.D., Wu, H.C., and Rick, P.D. (1997). A Salmonella typhimurium genetic locus which confers copper tolerance on copper-sensitive mutants of Escherichia coli. J. Bacteriol. *179*, 4977–4984. https://doi.org/10.1128/jb.179.16.4977-4984.1997.
18. Petit, G.A., Hong, Y., Djoko, K.Y., Whitten, A.E., Furlong, E.J., McCoy, A.J., Gulbis, J.M., Totsika, M., Martin, J.L., and Halili, M.A. (2022). The suppressor of copper sensitivity protein C from Caulobacter crescentus is a trimeric disulfide isomerase that binds copper (I) with subpicomolar affinity. Acta Crystallogr. D Struct. Biol. *78*, 337–352.
19. Shepherd, M., Heras, B., Achard, M.E.S., King, G.J., Argente, M.P., Kurth, F., Taylor, S.L., Howard, M.J., King, N.P., Schembri, M.A., and McEwan, A.G. (2013). Structural and functional characterization of ScsC, a periplasmic thioredoxin-like protein from Salmonella enterica serovar Typhimurium. Antioxidants Redox Signal. *19*, 1494–1506. https://doi.org/10.1089/ars.2012.4939.
20. Furlong, E.J., Lo, A.W., Kurth, F., Premkumar, L., Totsika, M., Achard, M.E.S., Halili, M.A., Heras, B., Whitten, A.E., Choudhury, H.G., et al. (2017). A shape-shifting redox foldase contributes to Proteus mirabilis copper resistance. Nat. Commun. *8*, 16065. https://doi.org/10.1038/ncomms16065.
21. Cho, S.-H., Parsonage, D., Thurston, C., Dutton, R.J., Poole, L.B., Collet, J.-F., Beckwith, J., and Maloy, S. (2012). A New Family of Membrane Electron Transporters and Its Substrates, Including a New Cell Envelope Peroxiredoxin, Reveal a Broadened Reductive Capacity of the Oxidative Bacterial Cell Envelope. mBio *3*, e00291-11. https://doi.org/10.1128/mBio.00291-11.
22. Subedi, P., Paxman, J.J., Wang, G., Hor, L., Hong, Y., Verderosa, A.D., Whitten, A.E., Panjikar, S., Santos-Martin, C.F., Martin, J.L., et al. (2021). *Salmonella enterica* BcfH is a trimeric thioredoxin-like bifunctional enzyme with both thiol oxidase and disulfide isomerase activities. Antioxidants Redox Signal. *35*, 21–39. https://doi.org/10.1089/ars.2020.8218.
23. López, C., Checa, S.K., and Soncini, F.C. (2018). CpxR/CpxA Controls scsABCD Transcription To Counteract Copper and Oxidative Stress in Salmonella enterica Serovar Typhimurium. J. Bacteriol. *200*, e00126-18. https://doi.org/10.1128/jb.00126-18.
24. Subedi, P., Paxman, J.J., Wang, G., Ukuwela, A.A., Xiao, Z., and Heras, B. (2019). The Scs disulfide reductase system cooperates with the metallochaperone CueP in Salmonella copper resistance. J. Biol. Chem. *294*, 15876–15888. https://doi.org/10.1074/jbc.RA119.010164.
25. Guddat, L.W., Bardwell, J.C., and Martin, J.L. (1998). Crystal structures of reduced and oxidized DsbA: investigation of domain motion and thiolate stabilization. Structure *6*, 757–767. https://doi.org/10.1016/s0969-2126(98)00077-x.
26. Emsley, P., and Cowtan, K. (2004). Coot: model-building tools for molecular graphics. Acta Crystallogr. D Biol. Crystallogr. *60*, 2126–2132. https://doi.org/10.1107/s0907444904019158.
27. Hiniker, A., Ren, G., Heras, B., Zheng, Y., Laurinec, S., Jobson, R.W., Stuckey, J.A., Martin, J.L., and Bardwell, J.C.A. (2007). Laboratory evolution of one disulfide isomerase to resemble another. Proc. Natl. Acad. Sci. USA *104*, 11670–11675. https://doi.org/10.1073/pnas.0704692104.
28. Santos-Martin, C., Wang, G., Subedi, P., Hor, L., Totsika, M., Paxman, J.J., and Heras, B. (2021). Structural bioinformatic analysis of DsbA proteins and their pathogenicity associated substrates. Comput. Struct. Biotechnol. J. *19*, 4725–4737. https://doi.org/10.1016/j.csbj.2021.08.018.
29. Banaszak, K., Mechin, I., Frost, G., and Rypniewski, W. (2004). Structure of the reduced disulfide-bond isomerase DsbC from Escherichia coli. Acta

Crystallogr. D Biol. Crystallogr. *60*, 1747–1752. https://doi.org/10.1107/S0907444904018359.

30. Zhao, Z., Peng, Y., Hao, S.-F., Zeng, Z.-H., and Wang, C.-C. (2003). Dimerization by Domain Hybridization Bestows Chaperone and Isomerase Activities. J. Biol. Chem. *278*, 43292–43298. https://doi.org/10.1074/jbc.M306945200.

31. Bader, M.W., Hiniker, A., Regeimbal, J., Goldstone, D., Haebel, P.W., Riemer, J., Metcalf, P., and Bardwell, J.C. (2001). Turning a disulfide isomerase into an oxidase: DsbC mutants that imitate DsbA. EMBO J. *20*, 1555–1562. https://doi.org/10.1093/emboj/20.7.1555.

32. Segatori, L., Paukstelis, P.J., Gilbert, H.F., and Georgiou, G. (2004). Engineered DsbC chimeras catalyze both protein oxidation and disulfide-bond isomerization in Escherichia coli: Reconciling two competing pathways. Proc. Natl. Acad. Sci. USA *101*, 10018–10023. https://doi.org/10.1073/pnas.0403003101.

33. Leverrier, P., Declercq, J.-P., Denoncin, K., Vertommen, D., Hiniker, A., Cho, S.-H., and Collet, J.-F. (2011). Crystal structure of the outer membrane protein RcsF, a new substrate for the periplasmic protein-disulfide isomerase DsbC. J. Biol. Chem. *286*, 16734–16742.

34. Majdalani, N., Heck, M., Stout, V., and Gottesman, S. (2005). Role of RcsF in signaling to the Rcs phosphorelay pathway in Escherichia coli. J. Bacteriol. *187*, 6770–6778. https://doi.org/10.1128/jb.187.19.6770-6778.2005.

35. Castanié-Cornet, M.P., Cam, K., and Jacq, A. (2006). RcsF is an outer membrane lipoprotein involved in the RcsCDB phosphorelay signaling pathway in Escherichia coli. J. Bacteriol. *188*, 4264–4270. https://doi.org/10.1128/jb.00004-06.

36. Dailey, F.E., and Berg, H.C. (1993). Mutants in disulfide bond formation that disrupt flagellar assembly in Escherichia coli. Proc. Natl. Acad. Sci. USA *90*, 1043–1047.

37. Hizukuri, Y., Yakushi, T., Kawagishi, I., and Homma, M. (2006). Role of the intramolecular disulfide bond in FlgI, the flagellar P-ring component of Escherichia coli. J. Bacteriol. *188*, 4190–4197. https://doi.org/10.1128/JB.01896-05.

38. Verderosa, A.D., Dhouib, R., Hong, Y., Anderson, T.K., Heras, B., and Totsika, M. (2021). A high-throughput cell-based assay pipeline for the preclinical development of bacterial DsbA inhibitors as antivirulence therapeutics. Sci. Rep. *11*, 1569. https://doi.org/10.1038/s41598-021-81007-y.

39. Malojčić, G., Owen, R.L., Grimshaw, J.P.A., Brozzo, M.S., Dreher-Teo, H., and Glockshuber, R. (2008). A structural and biochemical basis for PAPS-independent sulfuryl transfer by aryl sulfotransferase from uropathogenic *Escherichia coli*. Proc. Natl. Acad. Sci. USA *105*, 19217–19222. https://doi.org/10.1073/pnas.0806997105.

40. Kwon, A.R., and Choi, E.C. (2005). Role of disulfide bond of arylsulfate sulfotransferase in the catalytic activity. Arch Pharm. Res. (Seoul) *28*, 561–565. https://doi.org/10.1007/bf02977759.

41. Grimshaw, J.P.A., Stirnimann, C.U., Brozzo, M.S., Malojcic, G., Grütter, M.G., Capitani, G., and Glockshuber, R. (2008). DsbL and DsbI Form a Specific Dithiol Oxidase System for Periplasmic Arylsulfate Sulfotransferase in Uropathogenic Escherichia coli. J. Mol. Biol. *380*, 667–680. https://doi.org/10.1016/j.jmb.2008.05.031.

42. Totsika, M., Heras, B., Wurpel, D.J., and Schembri, M.A. (2009). Characterization of two homologous disulfide bond systems involved in virulence factor biogenesis in uropathogenic Escherichia coli CFT073. J. Bacteriol. *191*, 3901–3908. https://doi.org/10.1128/JB.00143-09.

43. Furlong, E.J., Kurth, F., Premkumar, L., Whitten, A.E., and Martin, J.L. (2019). Engineered variants provide new insight into the structural properties important for activity of the highly dynamic, trimeric protein disulfide isomerase ScsC from Proteus mirabilis. Acta Crystallogr. D Struct. Biol. *75*, 296–307. https://doi.org/10.1107/s2059798319000081.

44. Dutton, R.J., Boyd, D., Berkmen, M., and Beckwith, J. (2008). Bacterial species exhibit diversity in their mechanisms and capacity for protein disulfide bond formation. Proc. Natl. Acad. Sci. USA *105*, 11933–11938. https://doi.org/10.1073/pnas.0804621105.

45. Rozhkova, A., Stirnimann, C.U., Frei, P., Grauschopf, U., Brunisholz, R., Grütter, M.G., Capitani, G., and Glockshuber, R. (2004). Structural basis and kinetics of inter- and intramolecular disulfide exchange in the redox catalyst DsbD. EMBO J. *23*, 1709–1719. https://doi.org/10.1038/sj.emboj.7600178.

46. Totsika, M. (2017). Disarming pathogens: benefits and challenges of antimicrobials that target bacterial virulence instead of growth and viability. Future Med. Chem. *9*, 267–269. https://doi.org/10.4155/fmc-2016-0227.

47. Chant, A., Kraemer-Pecore, C.M., Watkin, R., and Kneale, G.G. (2005). Attachment of a histidine tag to the minimal zinc finger protein of the Aspergillus nidulans gene regulatory protein AreA causes a conformational change at the DNA-binding site. Protein Expr. Purif. *39*, 152–159.

48. Majorek, K.A., Kuhn, M.L., Chruszcz, M., Anderson, W.F., and Minor, W. (2014). Double trouble—Buffer selection and His-tag presence may be responsible for nonreproducibility of biomedical experiments. Protein Sci. *23*, 1359–1368. https://doi.org/10.1002/pro.2520.

49. Booth, W.T., Schlachter, C.R., Pote, S., Ussin, N., Mank, N.J., Klapper, V., Offermann, L.R., Tang, C., Hurlburt, B.K., and Chruszcz, M. (2018). Impact of an N-terminal Polyhistidine Tag on Protein Thermal Stability. ACS Omega *3*, 760–768. https://doi.org/10.1021/acsomega.7b01598.

50. Araújo, A.P., Oliva, G., Henrique-Silva, F., Garratt, R.C., Cáceres, O., and Beltramini, L.M. (2000). Influence of the histidine tail on the structure and activity of recombinant chlorocatechol 1,2-dioxygenase. Biochem. Biophys. Res. Commun. *272*, 480–484. https://doi.org/10.1006/bbrc.2000.2802.

51. Studier, F.W., and Moffatt, B.A. (1986). Use of bacteriophage T7 RNA polymerase to direct selective high-level expression of cloned genes. J. Mol. Biol. *189*, 113–130. https://doi.org/10.1016/0022-2836(86)90385-2.

52. Martinez, E., Bartolomé, B., and de la Cruz, F. (1988). pACYC184-derived cloning vectors containing the multiple cloning site and lacZα reporter gene of pUC8/9 and pUC18/19 plasmids. Gene *68*, 159–162.

53. Wang, R.F., and Kushner, S.R. (1991). Construction of versatile low-copy-number vectors for cloning, sequencing and gene expression in Escherichia coli. Gene *100*, 195–199.

54. Datsenko, K.A., and Wanner, B.L. (2000). One-step inactivation of chromosomal genes in Escherichia coli K-12 using PCR products. Proc. Natl. Acad. Sci. USA *97*, 6640–6645. https://doi.org/10.1073/pnas.120163297.

55. Cherepanov, P.P., and Wackernagel, W. (1995). Gene disruption in Escherichia coli: TcR and KmR cassettes with the option of Flp-catalyzed excision of the antibiotic-resistance determinant. Gene *158*, 9–14. https://doi.org/10.1016/0378-1119(95)00193-a.

56. Stols, L., Gu, M., Dieckman, L., Raffen, R., Collart, F.R., and Donnelly, M.I. (2002). A new vector for high-throughput, ligation-independent cloning encoding a tobacco etch virus protease cleavage site. Protein Expr. Purif. *25*, 8–15. https://doi.org/10.1006/prep.2001.1603.

57. Jarrott, R., Shouldice, S.R., Guncar, G., Totsika, M., Schembri, M.A., and Heras, B. (2010). Expression and crystallization of SeDsbA, SeDsbL and SeSrgA from Salmonella enterica serovar Typhimurium. Acta Crystallogr., Sect. F: Struct. Biol. Cryst. Commun. *66*, 601–604. https://doi.org/10.1107/s1744309110011942.

58. Hong, Y., and Reeves, P.R. (2014). Diversity of O-antigen repeat-unit structures can account for the substantial sequence variation in Wzx translocases. J. Bacteriol. *196*, 1713–1722.

59. Klebe, R.J., Harriss, J.V., Sharp, Z.D., and Douglas, M.G. (1983). A general method for polyethylene-glycol-induced genetic transformation of bacteria and yeast. Gene *25*, 333–341. https://doi.org/10.1016/0378-1119(83)90238-x.

60. Thomason, L.C., Costantino, N., and Court, D.L. (2007). E. coli genome manipulation by P1 transduction. Curr. Protoc. Mol. Biol. *1*, 1–17. https://doi.org/10.1002/0471142727.mb0117s79.

61. Obadia, B., Lacour, S., Doublet, P., Baubichon-Cortay, H., Cozzone, A.J., and Grangeasse, C. (2007). Influence of tyrosine-kinase Wzc activity on colanic acid production in Escherichia coli K12 cells. J. Mol. Biol. *367*, 42–53. https://doi.org/10.1016/j.jmb.2006.12.048.

62. Denoncin, K., Nicolaes, V., Cho, S.H., Leverrier, P., and Collet, J.F. (2013). Protein disulfide bond formation in the periplasm: determination of the *in vivo* redox state of cysteine residues. Methods Mol. Biol. *966*, 325–336. https://doi.org/10.1007/978-1-62703-245-2_20.

63. Studier, F.W. (2005). Protein production by auto-induction in high-density shaking cultures. Protein Expr. Purif. *41*, 207–234. https://doi.org/10.1016/j.pep.2005.01.016.

64. Lebowitz, J., Lewis, M.S., and Schuck, P. (2002). Modern analytical ultracentrifugation in protein science: a tutorial review. Protein Sci. *11*, 2067–2079. https://doi.org/10.1110/ps.0207702.

65. Schuck, P., Perugini, M.A., Gonzales, N.R., Howlett, G.J., and Schubert, D. (2002). Size-distribution analysis of proteins by analytical ultracentrifugation: strategies and application to model systems. Biophys. J. *82*, 1096–1111. https://doi.org/10.1016/s0006-3495(02)75469-6.

STAR★METHODS

KEY RESOURCES TABLE

REAGENT or RESOURCE	SOURCE	IDENTIFIER
Antibodies		
α-EcDsbA (Rabbit)	Makrina Totsika	
α-GroEL (Rabbit)	Invitrogen	PA5-144463
α-PmScsC (Rabbit)	Jennifer Martin	
a-Rabbit IgG (Goat antibody - conjugated to HRP)	Abcam	ab6721
α-SurA (Rabbit)	Renato Morona	
Chemicals, peptides, and recombinant proteins		
4′-acetamido-4′-maleimidylstilbene-2,2′-disulfonic acid	ThermoFisher Scientific	A485
1,4-Dithiothreitol	Roche	10708984001
Acetone	Sigma Aldrich	270725-1L
Bacto™ Casamino acids	BD	223050
Difco™ Agar	BD	214010
Ethylenediaminetetra-acetic acid di-sodium salt	Ajax Finechem	180-500G
Isopropyl β- d-1-thiogalactopyranoside	Sigma Aldrich	15502-5G
Phenol solution	Sigma Aldrich	P4557-100ML
Potassium 4-methylumbelliferyl sulfate	Sigma Aldrich	M7133
Potassium dihydrogen phosphate	Sigma Aldrich	7778-77-0
Sodium phosphate dibasic	Sigma Aldrich	S0876-500G
Sucrose	Chem-supply	SA030-5KG
Sulfuric acid (95-97 %)	Sigma Aldrich	1007320510
Trichloroacetic acid	Sigma Aldrich	T6399
Tris(hydroxymethyl)-aminomethane	Formedium	TRIS01

EXPERIMENTAL MODEL AND STUDY PARTICIPANT DETAILS

The *E. coli* bacterial strains and plasmids used in this study are described in Tables 1 and 2, respectively. In this work, the *E. coli* strains were grown at 37°C in LB-Lennox (5 g L^{-1} NaCl, 5 g L^{-1} yeast extract, 10 g L^{-1} tryptone) or on agar plates (LB with 15 g L^{-1} agar) unless otherwise indicated and specified in relevant assay conditions. Wherever appropriate, antibiotics were added at the following concentrations: ampicillin (100 μg mL^{-1}), kanamycin (50 μg mL^{-1}), and chloramphenicol (17 μg mL^{-1}).

METHOD DETAILS

Bacterial genetics methods

PmScsC-EcDsbA chimera was generated by Gibson assembly. The catalytic domains of *E. coli* DsbA (EcDsbA^{Cat}) was amplified by polymerase chain reaction (PCR) using the primers described in Table S1. The previously reported pMCSG7-PmScsC construct[20] was used as the template for PCR amplification of the N-terminal trimerization domain of PmScsC using the primers shown in Table S1. The gene encoding the PmScsC-EcDsbA chimera was amplified with NcoI-Pm*scsC* (Δss) Forward, and HindIII-EcDsbA Reverse (Table S1) from the expression construct into pSC108[21] so that the chimera carries an inframe DsbA signal sequence to aid the translocation of the protein. The resultant DsbAss–Δss(PmscsC)-PmscsC-EcDsbA chimera was then subcloned into the BamHI/HindIII sites of pSU2718.[52] The *C. crescentus scsC* gene (with *E. coli* DsbA signal sequence) was amplified from pSC108 (DsbAss-CcScsC)[21] with BamHI-Ec*dsbA* Forward and HindIII-Cc*scsC* Reverse (see Table S1) and cloned into pSU2718.[52] The *S. enterica scsC* gene was directly digested from pWSK29-StScsC[19] and subcloned into the BamHI/PstI restriction sites of pSU2718.[52] Knockout mutations in this work were constructed using a modified version of the Datsenko and Wanner method.[54,58] Early log phase cultures were induced with 10 mM L-arabinose for 40 min. Growth is immediately stopped by the addition of 2 × volumes of ice-cold 10% glycerol. The cell pellet is then collected and washed twice with ice-cold 10% glycerol and electroporated with 1.5 μg allelic replacement cassettes generated by PCR. Wherever appropriate, the selection cassettes used for gene knockouts were cleaved by the expression of Flp recombinase.[55] For plasmid transformations, early log phase cultures were pelleted and resuspended in a modified form of ice-cold TSS buffer (LB containing 10% w/v PEG 6000, 5% v/v DMSO,

20 mM $MgCl_2$, 20 mM $MgSO_4$, pH 6.5).[59] Plasmid DNA was then added and incubated on ice for 30 min. Nine volumes of LB were then added, and the cells were collected and plated onto selective media after 40 min. The transfer of chromosomal genetic traits between strains was performed by P1 transductions.[60] For the oligonucleotides used in cloning, gene replacements and screenings, see supplemental information (Table S1).

Swimming motility assay

Bacterial swimming motility was measured in 24-well plates.[38] Overnight 24 hr static cultures were normalized to OD_{600} 1.0 ($\sim 1 \times 10^9$ CFU/mL) and inoculated at the left-hand side of wells containing 0.25% w/v LB-Lennox agar (Gibco™ Bacteriological agar) supplemented with IPTG (500 μM) and chloramphenicol (17 μg mL^{-1}) that had been left to set and then dried overnight at room temperature (21°C). As bacteria radially migrated through the soft agar, a radial zone of motility corresponding to an increase in absorbance at 600 nm was observed, and a swimming motility curve was generated by tracking OD_{600} in a CLARIOstar plate reader (BMG, Australia) at 37°C over 20 hrs.

ASST sulfotransferase assay

Sulfotransferase activity was measured from overnight-grown liquid cultures.[38] Bacterial strains carrying the ASST construct were cultured in LB-Lennox media at 37°C overnight with 200 rpm aeration in the presence of IPTG (500 μM), ampicillin (100 μg mL^{-1}) and chloramphenicol (17 μg mL^{-1}). The cultures were washed once in 1× PBS, normalized to OD_{600} 0.8 ($\sim 7 \times 10^8$ CFU mL^{-1}) and transferred 100 μL per well into a Costar® 96-well plate. Cultures were mixed with an equal volume of 1× PBS solution containing 1 mM potassium 4-methylumbelliferyl sulfate (SIGMA ALDRICH, Castle Hill, Australia) and 2 mM phenol (SIGMA ALDRICH, Australia). Sulfotransferase activity was monitored in a CLARIOstar plate reader (BMG, Australia) over a 90 min period by measuring the fluorescence emitted at 450–480 nm (excitation wavelength at 360–380 nm).

Mucoidal colony morphology assay to track colanic acid production

Disulfide isomerase activity by ScsC proteins was determined phenotypically by enhanced production of colanic acid in *E. coli* K-12.[33] Briefly, single bacterial colonies were patched onto 1.5% solid agar M9 minimal media (2 μM $MgSO_4$, 100 nM $CaCl_2$, 0.4% v/v glycerol and 0.1% w/v casamino acid) containing IPTG (500 μM), and wherever appropriate, relevant antibiotics were added to maintain plasmids. The Cold Spring Harbor Protocol formula for M9 salts was used in this study (10× stock, per L, 70 g $Na_2HPO_4 \cdot 7H_2O$, 30 g KH_2PO_4, 5 g NaCl, 10 g NH_4Cl). Agar plates were incubated at 29°C for 48 hrs and macroscopically visualised for mucoidal colony morphology. Images were taken using a ChemiDoc MP Imaging System (Bio-Rad). For colanic acid quantification, the cells harvested were resuspended into 1× PBS and adjusted to OD_{600} 5.0. The samples were boiled for 15 min; then the supernatant was collected after 30 min centrifugation (15,000× G). The extracellular components were precipitated in 3× volumes of absolute ethanol overnight. The precipitants were collected by centrifugation and washed 1× in ice-cold absolute ethanol.

Colanic acid quantification

Colanic acid was quantified by reacting the isolated exopolysaccharides with concentrated sulfuric acid.[61] Cells were collected from the agar plates and resuspended in 1× PBS to give suspensions of OD_{600} 10. Equivalent volumes of samples (250 μL) were then incubated at 100°C for 15 mins. The supernatant was collected, mixed with 3× volumes of absolute ethanol and incubate at 5°C overnight. The precipitated exopolysaccharide was collected by centrifugation at 5°C and washed once with ice-cold absolute ethanol. The final sample was resuspended in 100 μL ddH_2O. Sulfuric acid (95-97 %) was diluted with ddH_2O at 6:1 v/v ratio. For quantification, each sample (10 μL) was mixed with the diluted sulfuric acid stock (900 μL) in glass vials and incubated at 100°C for 20 min. Each sample was then divided into two equal lots, one mixed 4.4 μL 1 M cysteine hydrochloride (prepared in 1M HCl) and another with equivalent volumes of 1 M HCl. Absorbance at 396 nm and 427 nm was measured in CLARIOstar plate reader (BMG, Australia). The readings from HCl controls were subtracted from the cysteine measurements to give ΔA396 and ΔA427 values. ΔA427 was then subtracted from ΔA396 values to give relative levels of exopolysaccharides. Noise generated from non-colanic acid contents in the extraction was removed with the use of an *E. coli* K-12 Δ*wcaJ* sample.

Labelling free cysteines groups, periplasmic extractions, and Western blot

Cell pellets equivalent to 1 mL OD_{600} 2.0 were harvested from late log phase cultures grown in M9 minimal media containing IPTG (500 μM) and relevant antibiotics. The cell pellet is first washed with 1× PBS and resuspended in ice-cold reaction buffer (50 mM Tris-HCl, pH 7.5, 0.1% v/v SDS and 10 mM EDTA). The free cysteine residues were labelled with 20 mM 4′-acetamido-4′-maleimidylstilbene-2,2′-disulfonic acid (AMS) in reaction buffer with reference to unlabelled controlled.[62] An additional control sample was first treated with DTT (10 mM) at 37°C for 5 min to fully reduce the proteins before AMS labelling. After the mixing with reaction buffers either with or without AMS, the samples are vortex rigorously for 1 min, and then incubated in the dark at 37°C for 1 hr. The samples were then resuspended in β-mercaptoethanol-free Lugtenburg buffer and used directly in Western blot.

For periplasmic extractions, the samples were resuspended in 500 μL ice-cold extraction buffer (20 mM Tris-HCl pH8, 20% w/v sucrose, 1 mM EDTA, 1 mg/mL lysozyme) and incubated on ice for 1 hr. The periplasmic fraction, which is present in the supernatant is then collected by centrifugation at 4°C (2 min at 15,000× G). Ice-cold trichloroacetic acid (100% w/v) was added to the collected supernatant to the final concentration of 20% v/v to precipitate the periplasmic content. The samples were then subjected to AMS

labelling as described earlier. The samples were then washed in 100% ice-cold acetone to dry and resuspended in β-mercaptoethanol-free Lugtenburg buffer. Wherever relevant, the SDS content in β-mercaptoethanol-free Lugtenburg buffer would be adjusted according to sample requirements and this is indicated on relevant result figures.

The samples were separated on 4–20% Mini-PROTEAN® TGX™ Precast Protein Gels and transferred by Trans-Blot Turbo Transfer System according to BIO-RAD instructions. The primary and secondary antibodies were used at the following dilutions, α-EcDsbA (1:5000), α-PmScsC (1:2000), α-SurA (1:10,000), α-GroEL (1:100,000), and HRP-conjugated α-Rabbit IgG (1:1,000).

Purification of PmScsC-EcDsbA chimera

Large scale expression of PmScsC-EcDsbA chimera was carried out by in *E. coli* BL21(DE3) in ZYM-5052 autoinduction media.[63] The cultures were incubated at 37°C for 4 h with 180 rev min^{-1} agitation, followed by incubation at 30°C for 18 hr with 180 rev min^{-1} agitation. PmScsC-EcDsbA was initially purified by immobilized metal affinity chromatography (IMAC) using a 5 mL HisTrap Fast Flow column (GE Healthcare) followed by cleavage of the N-terminal His_6-tag with TEV protease and reverse IMAC. The chimera was purified to homogeneity by size exclusion chromatography.

Protein biophysical characterisation

Analysis of protein secondary structure of PmScsC-EcDsbA was conducted by circular dichroism (CD) spectroscopy with an AVIV Model 410SF circular dichroism spectrophotometer (Aviv Biomedical, Inc) using a 1 mm quartz cuvette. 200 μg ml^{-1} of oxidised or reduced protein was prepared in 20 mM sodium phosphate, 0.1 mM EDTA, pH 7, with reduced protein samples supplemented with 0.75 mM DTT. Wavelength scans at 196–250 nm were conducted at 20°C and the CD signal from each protein scan were buffer subtracted and converted to molar ellipticity ($\Delta\varepsilon$ (M^{-1} cm^{-1}). Analytical size exclusion chromatography was performed with 5 mg of EcDsbA, BcfH (a trimeric Dsb protein) or PmScsC-EcDsbA [1.25 mg ml^{-1}] using a Superdex® 200 Increase 10/300 GL column equilibrated with 25mM HEPES pH 6.5, 150 mM NaCl. Elution profiles were determined by measuring absorbance at 280 nm. Sedimentation velocity analytical ultracentrifugation (SV-AUC) was used to confirm the oligomerization state of the chimera PmScsC-EcDsbA. SV-AUC was performed at 20°C using a Beckman Optima XL-A analytical ultracentrifuge using a conventional double-sector quartz cell mounted in an 8-hole An-50 Ti rotor. SV-AUC experiments were conducted using 380 μL of 2 mg ml^{-1} protein and 400 μL of reference solution consisting of 25 mM HEPES, 150 mM NaCl, pH 7.0. SV-AUC was run at 40,000 rpm, and scans were collected in a continuous mode at 285 nm. The partial specific volume, solvent density and viscosity were computed using SEDNTERP[64] and data was fitted using SEDFIT.[65]

QUANTIFICATION AND STATISTICAL ANALYSIS

The quantitative data and statistical tests in this work were plotted and analysed in GraphPad Prism 10 for macOS. The specific statistical tests, parameters, and *p*-values are reported in relevant figure legends.